Single Edge Position Modulation as a Dimming Technique for Visible Light Communications

Nobby Stevens, *Member, IEEE*, and Lieven De Strycker, *Member, IEEE*

***Abstract*—In this paper, a power switched, baseband modulation technique for visible light communications (VLC) is proposed and a theoretical model is constructed. It is shown that this technique, called single edge position modulation (SEPM), offers the unique performance characteristic that the communication properties reliability and power and spectral efficiency are invariable over a wide range of dimming levels. It is demonstrated that dimming robustness is obtained by increasing the number of bits per symbol. SEPM is compared with contemporary used baseband power switched modulation techniques for VLC that support dimming. The number of bits per symbol can be chosen to make a compromise between the dimming range over which reliability robustness is obtained on one hand, and the level of power and spectral efficiency on the other hand.**

***Index Terms*—Modulation, Monte Carlo simulation, reliability, synchronization, visible light communications.**

I. Introduction

DUE to the ubiquity of light emitting diodes (LEDs) for illumination and information panel lighting purposes, visible light communications (VLC) is a promising technology to meet the increasing demand for communication bandwidth and the surge of personal wireless area networks. VLC has a wide range of applications in the short- and medium-range communication, as well in- as outdoors [1], [2]. Compared with radio frequency (RF)-technology, VLC has distinct properties such as a large unlicensed communication band, immunity for Electromagnetic Interference (EMI) and extra security due to its local character [3], [4].

VLC sends information by intensity modulating artificial light. For the development of a physical (PHY) layer for VLC, two important conditions must be taken into account in the design of modulation techniques [5]. These are the avoidance of flicker and the integration of the illumination dimming functionality. Flicker is the unwanted and human observable time variation in the light intensity. For static environments, flickering is negligible at frequencies above 200 Hz [6], but recent studies demonstrate that adverse effects can be observed at higher frequencies [7]. In this work, flickering is not studied in detail, but the method does allow flicker suppression. Dimming control is mandatory with LED lighting because it can provide moods and saves energy.

LEDs are current driven devices, where the light output is proportional to the forward current. There are two ways to control the brightness, namely by modifying the forward current (known as analogous dimming) or by modulating the width of a pulse in the time domain (known as pulse width modulation (PWM) or power switched dimming [8]). With analogous dimming, a change in current can lead to an unwanted wavelength shift of the emitted light (known as chromaticity shift [9]). With PWM, the nominal current is supplied but the dimming is accomplished by modifying the pulse width. Due to the potential wavelength shift in the current dimming method and the reduced hardware implementation cost, most LEDs use PWM as a means for dimming.

Several modulation schemes have been proposed for high- and low- data rate applications. Significant advances have been made in the IEEE 802.15.7 standard [5], [10]. This standard defines a PHY and medium access control (MAC) layer for different types of applications. PHY I and PHY II describe a single source link, making use of on-off keying (OOK) or variable pulse position modulation (VPPM). In the related task group (IEEE P802.15 Working Group for Wireless Personal Area Networks (WPANs)), variable on-off keying (VOOK) was proposed as a variant on OOK to achieve a wide range of dimming levels by introducing filler bits [11]. VOOK and VPPM are both power switched, dedicated baseband modulation forms to support simultaneously dimming and data communication. For these PHY layers, data rates from 11.67 kbps until 96 Mbps are possible when there is an optical bandwidth at the transmitter side from 200 kHz to 120 MHz. PHY III concerns the usage of multiple color sources [12]–[15]. Data rates from 12 Mbps to 96 Mbps can be established when red-green-blue (RGB) LEDs are used with an optical bandwidth of 12 MHz or 24 MHz.

Apart from VOOK and VPPM, no other dedicated, power switched, baseband modulation techniques for VLC that support simultaneously dimming and communication are published [8]. Multiple other baseband VLC modulation schemes were studied though, but they are not oriented towards dimming as VOOK or VPPM are, or apply analogues dimming in contrast to power switched dimming [16]–[27].

Besides previous baseband modulation forms, the use of discrete multitone modulation (DMT) schemes has been considered for high data rate applications [28]–[30]. Here, an analog front end at the LED driver is required, where in most cases a dc bias current is imposed. Scaling the bias current and more advanced techniques can be used to provide dimming support [31].

In this paper, the SEPM technique is elaborated. As already demonstrated by other authors for infrared communication [32], the presence or absence of an edge instead of a pulse in a power switched modulation scheme can be used to transmit information. In this work, it is demonstrated that this concept leads to an invariance of the communication

Manuscript received April 5, 2016; revised June 24, 2016, August 12, 2016, and September 28, 2016; accepted September 28, 2016. Date of publication October 2, 2016; date of current version November 17, 2016.

The authors are with the ESAT, Katholieke Universiteit Leuven, Ghent 9000, Belgium (e-mail: nobby.stevens@kuleuven.be; lieven.destrycker@kuleuven.be).

Digital Object Identifier 10.1109/JLT.2016.2614826

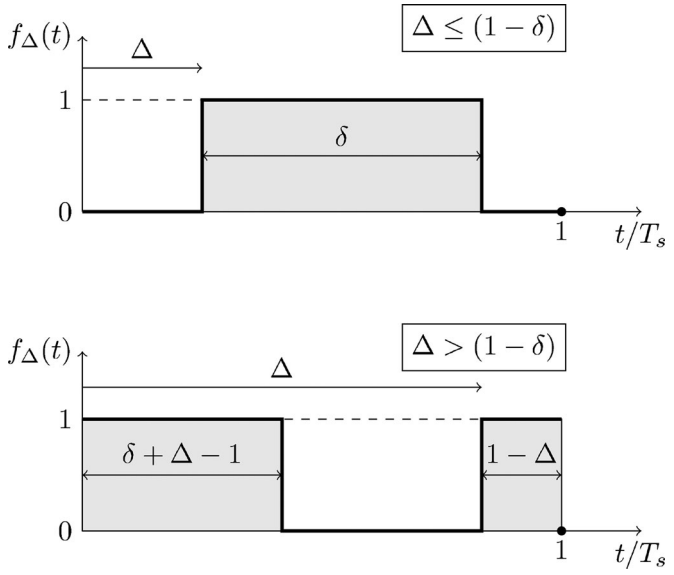

Fig. 1. Definition of $f_\Delta(t)$.

properties with regard to a well-defined range of dimming levels.

In Section II, the modulating wave form is explored and a theoretical expression for the error probability is obtained. Other communication performance parameters such as the power requirement, spectral efficiency and synchronization sensitivity are also considered. In Section III, SEPM is compared to the two other power switched, dimming supporting modulation forms (VOOK and VPPM). In the concluding Section IV, the main results of this work are summarized.

II. Communication Properties

A. Definition of the Modulating Waveform

Let us consider a waveform $f_\Delta(t)$, being defined during the symbol time T_s (see Fig. 1). $\delta \in]0,1[$ is the duty cycle and determines the dimming level, while the delay $\Delta \in [0,1[$ is the relative position (within T_s) of the rising edge that will be used to transmit information. $f_\Delta(t)$ is defined as in (1) and (2). If $\Delta \leq (1-\delta)$:

$$f_\Delta(t) = \begin{cases} 0 & t/T_s \in [0,\Delta[\\ 1 & t/T_s \in [\Delta, \Delta+\delta[\\ 0 & t/T_s \in [\Delta+\delta, 1] \end{cases} \quad (1)$$

If $\Delta > (1-\delta)$:

$$f_\Delta(t) = \begin{cases} 1 & t/T_s \in [0, \delta+\Delta-1[\\ 0 & t/T_s \in [\delta+\Delta-1, \Delta[\\ 1 & t/T_s \in [\Delta, 1] \end{cases} \quad (2)$$

This can be interpreted as follows. In (1) and (2), the rising edge is positioned at $t = \Delta T_s$. From that point in time, the level of the modulating wave form is set to 1 during δT_s. If δ is larger than $1-\Delta$, the remaining part where $f_\Delta(t)$ equals 1 is shifted to the beginning of the symbol time frame (see (2)). It is clear that if Δ equals 1, that this is identical with $\Delta = 0$. Therefore,

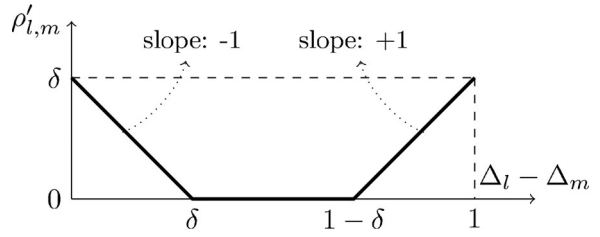

Fig. 2. Representative plot of the symbol time scaled correlation for $\delta \leq 0.5$ (in this graph, as an example $\delta = 0.3$).

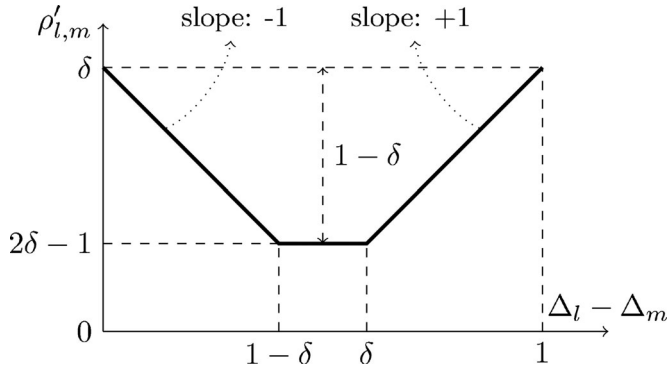

Fig. 3. Representative plot of the symbol time scaled correlation for $\delta \geq 0.5$ (in this graph, as an example $\delta = 0.6$).

we have limited the possible value range for Δ between 0 and 1, including 0 and excluding 1. The energy content $\mathcal{E}_s$ of $f_\Delta(t)$ is δT_s and thus independent of Δ. The symbol time scaled correlator $\rho'_{l,m}$ of two functions $f_{\Delta_l}(t)$ and $f_{\Delta_m}(t)$ evaluated at the symbol time (3) is shown on Figs. 2 and 3.

$$\rho'_{l,m} = \frac{1}{T_s}\int_0^{T_s} f_{\Delta_l}(t) f_{\Delta_m}(t) dt \quad (3)$$

A distinction has to be made between the cases where δ is larger or smaller than 0.5. The maximal difference in values for $\rho'_{l,m}$ is δ (for $\delta \leq 0.5$) or $(1-\delta)$ (for $\delta \geq 0.5$). An important observation that will be exploited later in this work, is that the slope of the piece wise linear dependencies of $\rho'_{l,m}$, equals ± 1, and is not depending on the duty cycle δ.

For digital communications, the number of possible messages is finite. Suppose that we have M possible values of Δ, where these values are uniformly distributed between 0 and 1 with 0 as the first value (4). This leads to the definition of a finite set of waveforms $f_m(t) = f_{\Delta_m}(t)$, with $m \in \{0,1,...,M-1\}$.

$$\Delta_m = \frac{m}{M}, \text{ with } m \in \{0,1,2,...,M-1\} \quad (4)$$

B. Reliability Characterization

On Fig. 4, an LED, traditionally used for illumination purposes with dimming functionality, receives a number m (with $m \in \{0,1,\cdots,M-1\}$) to be transmitted during symbol time T_s. The number m is associated with the waveform $f_m(t)$. The transmitted power $P_{Tx}(t)$ by the LED is modulated by $f_m(t)$. $P_{Tx}(t)$ is, within each symbol time, described by (5), where P_n

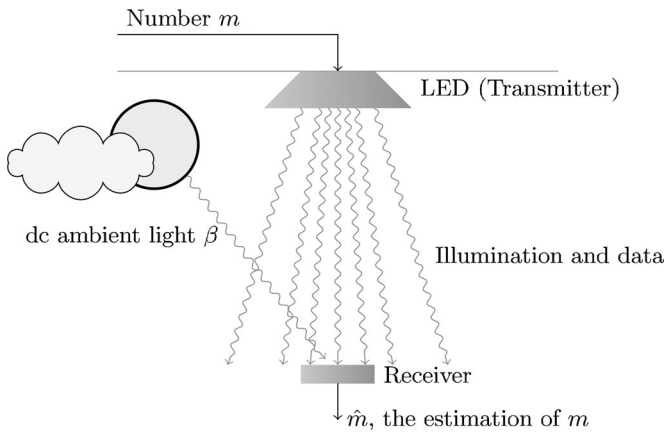

Fig. 4. Configuration under study.

is the power at the nominal current level.

$$P_{Tx}(t) = P_n \; f_m(t) \tag{5}$$

At the receiver, the impeding power is transformed into a signal $r(t)$ by an intensity based detector (photo diode). The signal $r(t)$ has the form of (6), with R the responsivity of the receiver, $H(0)$ the channel reponse, β the dc contribution from ambient light and $n(t)$ is a noise component that can be considered as a sample function of an additive white gaussian noise process [33]. The channel is represented as a flat function of the frequency and equals the dc channel response for the signals under consideration [34]. Remark that we suppose perfect symbol synchronization between the transmitter and receiver.

$$r(t) = RH(0) \; P_n \; f_m(t) + \beta + n(t) \tag{6}$$

The goal is to determine which m was transmitted, based on the signal $r(t)$. This estimated value is noted as $\hat{m}$, as shown on Fig. 4. We call $P = H(0) \; P_n$ the amount of power originated from the transmitter being switched on, that is captured by the detector. It is known that for a white gaussian noise process, the receiver that minimizes the error probability is implemented as an amplitude detection of the output of a signal correlator [35]. The output r_k of the k^{th} correlator sampled at T_s ($k \in \{0, 1, 2, ..., M-1\}$) can be written as in (7), with n_k the noise component contribution at the output of correlator k.

$$\begin{aligned} r_k &= \int_0^{T_s} r(t) f_k(t) dt \\ &= RPT_s \; \rho'_{k,m} + \beta \, \delta \, T_s + n_k \end{aligned} \tag{7}$$

The maximal value of $\rho'_{k,m}$ equals δ, and is valid for $k = m$ (see Figs. 2 and 3). Thus the detector must select the highest r_k, which leads to the maximal likelihood estimation of the original sent number m. The error rate is determined by the probability that there is an output value of at least one correlator that is higher than r_m. Let us consider the term n_k.

$$n_k = \int_0^{T_s} n(t) f_k(t) dt \tag{8}$$

We have that the expectation value $E[n_k] = 0$ and variance $E[n_k^2] = \delta \, T_s \; N_0$ with N_0 the unilateral power spectral density of the additive white gaussian process. Remark that the ambient light is taken into account in the time-invariant contribution β, making that the expectation value of the noise equals 0. In order to focus the attention and without loss of generality, we suppose that $m = 0$ was transmitted. The probability $\mathcal{P}$ that the output of correlator $k (\neq 0)$ is higher than r_0 is described by (9).

$$\begin{aligned} \mathcal{P}(r_k > r_0) = \; & \mathcal{P}\left[\left(RPT_s \; \rho'_{k,0} + n_k + \beta \, \delta \, T_s \right) \right. \\ & \left. > \left(RPT_s \; \delta + n_0 + \beta \, \delta \, T_s \right) \right] \\ = \; & \mathcal{P}\left[(n_k - n_0) \right. \\ & \left. > \left(RPT_s \; (\delta - \rho'_{k,0}) \right) \right] \end{aligned} \tag{9}$$

Since n_k and n_0 are both correlator outputs from an additive white gaussian process with zero mean and identical variance, $n_k - n_0$ is also a gaussian variable with zero mean. The variance of $n_k - n_0$ is derived in (10). Due to the, in general, non-orthogonality of the waveforms $f_0(t)$ and $f_k(t)$, $E[n_k n_0]$ is different from zero and equals $T_s \; \rho'_{k,0} \; N_0$.

$$\begin{aligned} E\left[(n_k - n_0)^2 \right] = \; & E\left[n_k^2 \right] + E\left[n_0^2 \right] - 2E\left[n_k n_0 \right] \\ = \; & 2 \, T_s \; N_0 \; \left(\delta - \rho'_{k,0} \right) \end{aligned} \tag{10}$$

This leads to expression (11) for $\mathcal{P}(r_k > r_0)$.

$$\mathcal{P}(r_k > r_0) = \mathrm{Q}\left(RP \sqrt{\frac{T_s \left(\delta - \rho'_{k,0} \right)}{2 \, N_0}} \right) \tag{11}$$

$\mathrm{Q}(x)$ is known as the q-function, and is a scaled version of the complementary error function ($\mathrm{Q}(x) = 0.5 \mathrm{erfc}(x/\sqrt{2})$). For the upper limit of the symbol error rate ($SER^{(U)}$), the union bound axiom [36] can be used, leading to expression (12).

$$SER \leq \sum_{k=1}^{M-1} \mathcal{P}(r_k > r_0) = SER^{(U)} \tag{12}$$

Depending on the dimming level range and the number of symbols M, two possibilities occur. First, suppose that we choose the number of possible symbols M high enough, so that the nearest symbols are in the sloping part of $\rho'_{k,0}$ over the entire dimming range. If $M = 8$ for instance, the nearest symbols for $m = 0$ are the symbols represented by $f_1(t)$ and $f_7(t)$, implying that $\delta - \rho'_{1,0} = \delta - \rho'_{7,0} = 8^{-1}$. This is illustrated on Fig. 5, where the discrete levels are shown for this example with $\delta = 0.6$. If the number M of possible symbols is high enough in order to have the nearest symbols in the sloping part of the symbol-averaged correlation, expression (13) for the symbol error rate SER is valid in the high signal to noise ratio scenario since $\delta - \rho'_{1,0} = \delta - \rho'_{M-1,0} = 1/M$. Remark that we have neglected the term $-\mathcal{P}(r_1 > r_0) \cdot \mathcal{P}(r_{M-1} > r_0)$.

$$\begin{aligned} SER = \; & \mathcal{P}(r_1 > r_0) + \mathcal{P}(r_{M-1} > r_0) \\ = \; & 2\mathrm{Q}\left(RP \sqrt{\frac{T_s}{2 \, N_0 \, M}} \right) \end{aligned} \tag{13}$$

When we consider the argument of the Q-function, we see that the error rate is independent on the dimming level. The necessary condition for reliability independence on the dimming, is that M

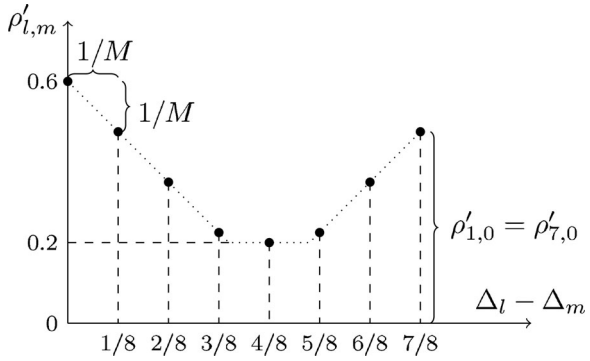

Fig. 5. $\rho'_{l,m}$ for $\delta = 0.6$ and $M = 8$.

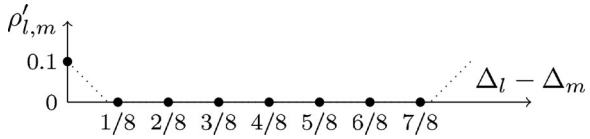

Fig. 6. $\rho'_{l,m}$ for $\delta = 0.1$ and $M = 8$.

must be chosen sufficiently high or the dimming range must be chosen sufficiently low so that the two nearest symbols are in the sloping part of the symbol time averaged correlation curve. As an example, suppose that the system allows dimming between 0.1 and 0.9. It is clear that $M = 8$ is not sufficient, since $1/8 > 0.1$. If $M = 16$ is chosen for δ to vary between 0.1 and 0.9, the reliability will be independent on the dimming level since the nearest symbols will be in the sloping part of $\rho'_{l,m}$. Applying Gray coding for the subsequent symbols, this leads to (14) for the bit error rate (BER) since every symbol time T_s, $\log_2(M)$ bits are transmitted.

$$BER = \frac{2}{\log_2(M)} \mathrm{Q}\left(RP\sqrt{\frac{\log_2(M)}{2\,M\,N_0\,R_b}}\right) \tag{14}$$

Here, R_b is the bit rate defined as in (15).

$$R_b = \frac{\log_2(M)}{T_s} \tag{15}$$

A second possibility that occurs is that the dimming level with regard to the numbers of bits per symbol is such that all the symbols are located in the flat part of the time averaged correlation curve. This is illustrated on Fig. 6, where a dimming level δ of 0.1 is applied with $\log_2(M) = 3$ bits. Remark that this condition this does not necessarily imply that the dimming level is low, as one can see on Fig. 7 where the dimming equals 0.9 for the same number of bits per symbol as in Fig. 6. As can be seen on Fig. 2 and Fig. 3, the distance to all the other symbols is equal and is δ in case $\delta \leq 0.5$ and $(1-\delta)$ for $\delta \geq 0.5$, leading to the definition of γ in (16).

$$\gamma = \begin{cases} \delta & \text{for} \quad \delta \leq 0.5 \\ 1-\delta & \text{for} \quad \delta \geq 0.5 \end{cases} \tag{16}$$

Based on (11) and (12), one can write that the symbol error rate is upper bound as in (17), when all other symbols are located in the flat part of the correlation curve.

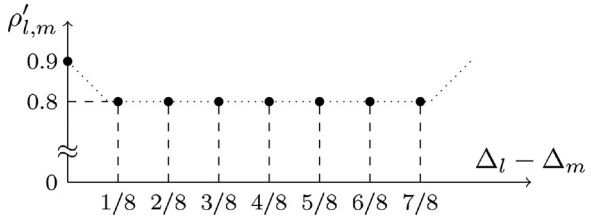

Fig. 7. $\rho'_{l,m}$ for $\delta = 0.9$ and $M = 8$.

$$\begin{aligned} SER^{(U)} &= (M-1)\mathcal{P}\left(r_k > r_0\right) \\ &= (M-1)\mathrm{Q}\left(RP\sqrt{\frac{T_s\,\gamma}{2\,N_0}}\right) \end{aligned} \tag{17}$$

Applying Gray coding, relationship (18) is valid. We have found that the sum of the difference bits over all possible symbols using Gray coding, divided by the number of bits $\log_2(M)$ equals $M/2$.

$$BER^{(U)}_{M,\gamma \leq 1/\mathrm{M}} = \frac{M}{2}\,\mathrm{Q}\left(RP\sqrt{\frac{\log_2(M)\,\gamma}{2\,R_b\,N_0}}\right) \tag{18}$$

C. Power Requirement and Spectral Efficiency

Regarding the power requirement, a distinction is needed between the situation where the nearest symbols are in the sloping part of the correlation or where all other symbols are found in the flat part of that curve. Using (14), we obtain relationship (19).

$$P = \frac{1}{R}\sqrt{\frac{2\,M\,N_0\,R_b}{\log_2(M)}}\mathrm{Q}^{-1}\left(\frac{\log_2(M)}{2}BER\right) \tag{19}$$

If all the other symbols are in the flat part of the correlation curve, (20) is valid.

$$P = \frac{1}{R}\sqrt{\frac{2\,N_0\,R_b}{\log_2(M)\,\gamma}}\mathrm{Q}^{-1}\left(\frac{2}{M}BER\right) \tag{20}$$

The spectral efficiency ν is defined as the amount of bits that is transmitted per Hertz required bandwidth. The symbol time T_s contains $\log_2(M)$ bits. The smallest possible pulse width according the definition of $f_m(t)$ is T_s/M, which leads to the spectral efficiency ν (21).

$$\nu = \frac{\log_2(M)}{M} \tag{21}$$

D. Synchronization Sensitivity

Several authors have addressed the impact of synchronization errors on the reliability for baseband optical communications [37], [38]. A rigorous treatment of the subject is beyond the scope of this work, but by means of Monte Carlo simulations avoiding extensive theoretical elaborations, a number of interesting conclusions can be drawn. Here, we consider the impact

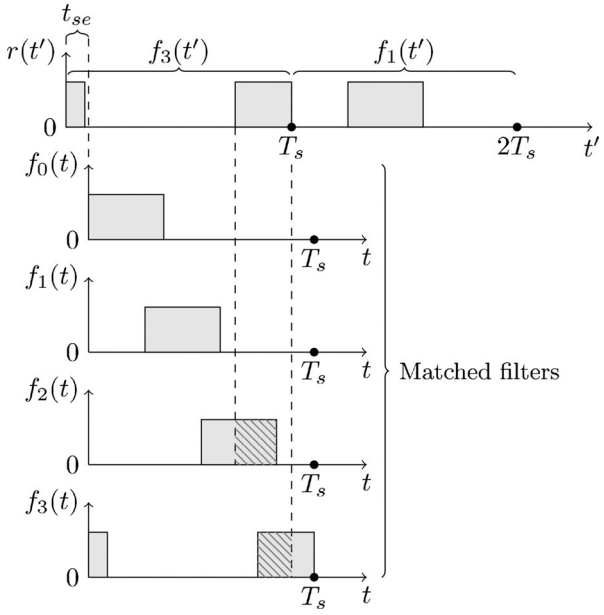

Fig. 8. Illustration of the synchronization error impact on the matched filter outputs r_k for $\delta = 0.33$, $t_{\rm se} = 0.1\,T_s$ and the transmitted wave forms f_3 and f_1. The hatched area shows the overlap of the matched filters with the received signal $r(t')$.

on the BER of a symbol synchronization offset between the receiver and transmitter.

In order to illustrate the phenomenon, we have chosen a dimming δ of 33 % with 2 bits per symbol, where the wave forms f_3 and f_1 are transmitted subsequently as shown on Fig. 8. In order to focus the attention, we did not include the dc and noise contribution. A synchronization offset $t_{\rm se} = t' - t$ of 10 % of the symbol time T_s is introduced. Relationship (22) can be applied to determine the occurrence of a symbol error caused by a synchronization offset. Remark that (22) equals (7) if $t_{\rm se} = 0$.

$$r_k = \int_0^{T_s - t_{\rm se}} r(t + t_{\rm se}) f_k(t) dt + \int_{T_s - t_{\rm se}}^{T_s} r(t + t_{\rm se}) f_k(t) dt \tag{22}$$

The value of the different matched filters is determined by two consecutive transmitted wave forms, where the second term of (22) is the contribution of the subsequent symbol. Considering the example, it is clear that when $t_{\rm se} = 0$, r_3 will correctly have the highest probability of being the largest filter output. With $t_{\rm se} = 0.1\,T_s$ though, r_2 will have the highest value, resulting in a BER of nearly 1 under low noise conditions. Remark that a situation where the matched filtering occurs too early instead of too late (as in our example) leads to an analogous reasoning, with identical conclusions. In order to gain insight in the influence of the subsequent wave form, let us suppose that instead of f_1, f_0 would have been submitted. In that case, r_3 would be the largest value since there would be an additional contribution from the next symbol frame.

Based on previous reasoning, it is clear that the number of bits per symbol $\log_2(M)$ and the dimming δ strongly influences the impact of $t_{\rm se}$ on the BER. In order to quantify this more accurately, we have performed a Monte Carlo simulation where

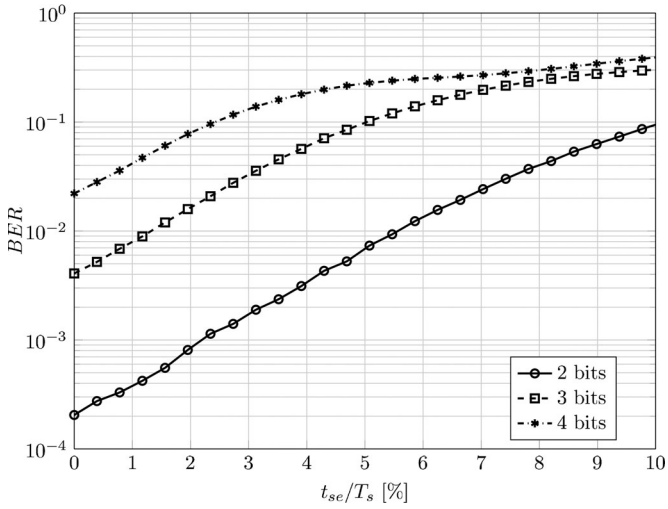

Fig. 9. Deterioration of the BER as a function of the relative synchronization error for 2, 3 and 4 bits per symbol with $\gamma = 0.5$.

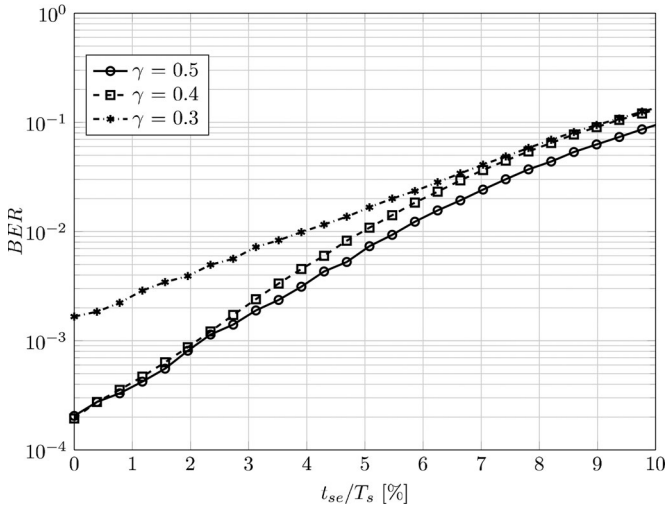

Fig. 10. Deterioration of the BER as a function of the relative synchronization error for 2 bits per symbol with varying γ.

a large number of randomly chosen symbols are transmitted with $t_{\rm se}$ as the independent variable, where the additive gaussian noise contribution $n(t)$ (see (6)) had a fixed N_0 and leading to a BER of 2 10^{-4} for 2 bits per symbol SEPM without synchronization error. The result can be found on Figs. 9 and 10. It can indeed be concluded that the higher the number of bits per symbol and the lower γ (as defined in (16)), the more critical the synchronization. Remark that it is rather γ that determines the sensitivity, a δ of 0.4 leads to the same result as a δ of 0.6.

III. Comparison With VOOK and VPPM

The power requirement and spectral efficiency for VOOK and VPPM have been described previously [39]. In order to compare the required power at the receiver side, the ratio of the required power with SEPM ($P_{\rm sepm}$) on the required power with VPPM $P_{\rm vppm} (= P_{\rm vook})$ is plotted for a BER of 10^{-6} on Fig. 11 in dB for $\log_2(M)$ equal to 2, 3 and 4 bits per symbol. It is clear

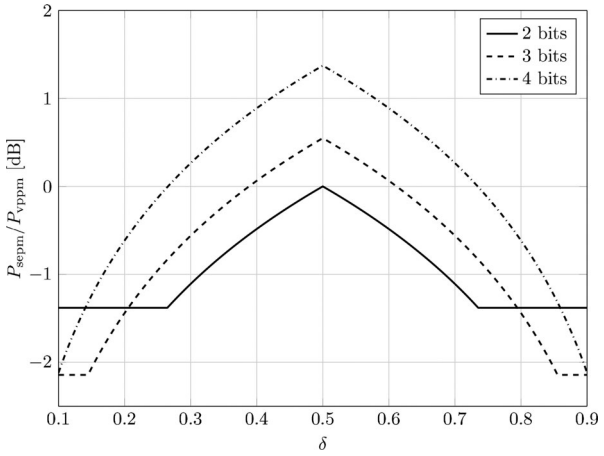

Fig. 11. Relative power requirement for $\log_2(M)$ bits per symbol.

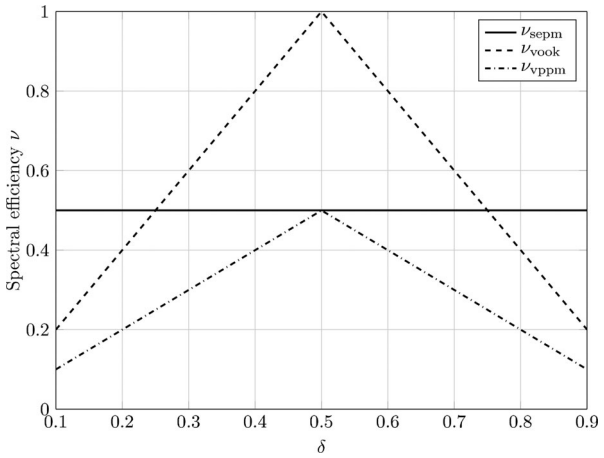

Fig. 12. Comparison of the spectral efficiency, where $\nu_{\text{sepm}} = 1/2$ when $\log_2(M) = 2$ bits.

that regarding the power efficiency, the usage of 2 bits per symbol leads to a more power efficient modulation scheme over the entire dimming range, while an increasing number of bits per symbol has a degrading influence on the power efficiency. The range over which the reliability is independent on the dimming is limited to $\delta \in [0.25, 0.75]$ using 2 bits per symbol. A higher number of bits per symbol increases this range, but clearly deteriorates the power efficiency. Remark that if only one bit per symbol is considered for SEPM, the reliability is identical to VPPM and VOOK.

In contrast to VPPM and VOOK, the spectral efficiency of SEPM is independent on the dimming δ. Based on (21), one can readily observe that the modulation scheme becomes less spectral efficient as the number of bits per symbol increases. For $\log_2(M) = 2$ bits, we have that $\nu_{\text{sepm}} = 1/2$. On Fig. 12, a comparison of the spectral efficiency is shown. SEPM using 2 bits per symbol has a better spectral efficiency than VPPM over the entire range, while VOOK is more spectral efficient for dimming levels between 0.25 and 0.75.

When comparing different power switched modulation schemes for VLC that support dimming, a number of criteria must be considered:

1) The power efficiency: The SEPM power efficiency depends on the number of symbols M, where the most optimal value is obtained as only 2 bits per symbol are used. SEPM is more power efficient than VPPM and VOOK over the entire dimming range.
2) The spectral efficiency: Here also, the most favorable number of bits per symbol using SEPM is 2. SEPM is more spectral efficient than VPPM over the entire range and better than VOOK for $\gamma \leq 0.25$.
3) The robustness of the reliability with regard to dimming: SEPM has the property to have a BER that is independent on the dimming value within a certain range determined by the number of bits per symbol. Using VOOK and VPPM, the reliability modifies significantly as the dimming changes. Unfortunately, when an extended reliability robust dimming range is required, a high number of bits per symbol is needed. This implies a decrease in power and spectral efficiency.
4) The hardware implementation complexity: A higher number of possible symbols leads to an increase of correlators at the receiver. Here also, the usage of 2 bits per symbol SEPM is advantageous.
5) Symbol synchronization: More bits per symbol will lead to the need of a more accurate symbol synchronization at the receiver.

Taking into account previous items, it is clear that a 2 bits per symbol SEPM modulation scheme is more favorable than VPPM and VOOK. It has higher power efficiency, a dimming independent and fair spectral efficiency and it has the unique property to have a reliability that is independent of the dimming for $\delta \in [0.25, 0.75]$. When the designer wants to enlarge the dimming range over which the reliability is constant, the number of bits per symbol needs to be increased. This is at the cost of a lower power and spectral efficiency, a more critical synchronization and an increase of the receiver complexity.

IV. Conclusion

In this work, the SEPM technique is presented. It is demonstrated that SEPM has the unique property that dimming over a specific range does not influence the reliability of the transmission in the high signal to noise ratio scenario. This dimming range is determined by the number of bits per symbol. The larger the number of bits per symbol, the larger this reliability invariant dimming range. The disadvantage of an increased number of bits per symbol is that the power efficiency and spectral efficiency both decrease, while the synchronization becomes more critical and the complexity of the receiver increases. SEPM is compared to the two other power switched modulation forms VOOK and VPPM. The communication properties for these techniques depend strongly on the amount of dimming, while with SEPM, a high degree of dimming robustness is obtained. SEPM using 2 bits per symbol delivers an improved power efficiency compared to VOOK and VPPM, and this over the entire dimming range. At low or high dimming levels, there is a higher spectral efficiency of 2 bits per symbol SEPM compared to VOOK, while with regard to VPPM, the spectral efficiency is always higher disregard the dimming level.

REFERENCES

[1] A. Jovicic, J. Li, and T. Richardson, "Visible light communication: Opportunities, challenges and the path to market," *IEEE Commun. Mag.*, vol. 51, no. 12, pp. 26–32, Dec. 2013.

[2] T. Yamazato *et al.*, "Image-sensor-based visible light communication for automotive applications,"*IEEE Commun. Mag.*, vol. 52, no. 7, pp. 88–97, Jul. 2014.

[3] H. Burchardt, N. Serafimovski, D. Tsonev, S. Videv, and H. Haas, "VLC: Beyond point-to-point communication," *IEEE Commun. Mag.*, vol. 52, no. 7, pp. 98–105, Jul. 2014.

[4] D. Karunatilaka, F. Zafar, V. Kalavally, and R. Parthiban, "Led based indoor visible light communications: State of the art," *IEEE Commun. Surveys Tuts.*, vol. 17, no. 3, pp. 1649–1678, thirdquarter 2015.

[5] S. Rajagopal, R. Roberts, and S.-K. Lim, "IEEE 802.15.7 visible light communication: Modulation schemes and dimming support," *IEEE Commun. Mag.*, vol. 50, no. 3, pp. 72–82, Mar. 2012.

[6] S. e. a. Barman, "Human electroretinogram responses to video displays, fluorescent lighting, and other high frequency sources," *Optometry Vis. Sci.*, vol. 68, no. 8, pp. 645–662, 1991.

[7] J. Bullough and D. Marcus, "Influence of flicker characteristics on stroboscopic effects," *Lighting Res. Technol.*, 2015, doi: 10.1177/1477153515599566.

[8] F. Zafar, D. Karunatilaka, and R. Parthiban, "Dimming schemes for visible light communication: The state of research," *IEEE Wireless Commun.*, vol. 22, no. 2, pp. 29–35, Apr. 2015.

[9] M. Dyble, N. Narendran, A. Bierman, and T. Klein, "Impact of dimming white LEDs: Chromaticity shifts due to different dimming methods," *Proc SPIE*, vol. 5941, pp. 291–299, Sep. 2005.

[10] E. Sarbazi and M. Uysal, "PHY layer performance evaluation of the IEEE 802.15.7 visible light communication standard," in *Proc. 2nd Int. Workshop Opt. Wireless Commun.*, Oct. 2013, pp. 35–39.

[11] S. Kaur, W. Liu, and D. Castor, "VLC dimming proposal," IEEE P 802.15 Working Group for wireless personal area networks (WPANs), Tech. Rep. 802.15-15-09-0641-00-0007, Sep. 2009.

[12] W. Popoola, E. Poves, and H. Haas, "Error performance of generalised space shift keying for indoor visible light communications," *IEEE Trans. Commun.*, vol. 61, no. 5, pp. 1968–1976, May 2013.

[13] R. Singh, T. O'Farrell, and J. David, "An enhanced color shift keying modulation scheme for high-speed wireless visible light communications," *J. Lightw. Technol.*, vol. 32, no. 14, pp. 2582–2592, Jul. 2014.

[14] R. Singh, T. O'Farrell, and J. David, "Performance evaluation of IEEE 802.15.7 CSK physical layer," in *Proc. IEEE Globecom Workshops*, Dec. 2013, pp. 1064–1069.

[15] F. Delgado Rajo, V. Guerra, J. Rabadan Borges, J. Rufo Torres, and R. Perez-Jimenez, "Color shift keying communication system with a modified PPM synchronization scheme," *IEEE Photon. Technol. Lett.*, vol. 26, no. 18, pp. 1851–1854, Sep. 2014.

[16] T. Ozaki, Y. Kozawa, and Y. Umeda, "Improved error performance of variable PPM for visible light communication," in *Proc. Int. Symp. Wireless Pers. Multimedia Commun. Symp.*, Sep. 2014, pp. 259–264.

[17] Z. Ghassemlooy, A. Hayes, N. Seed, and E. Kaluarachchi, "Digital pulse interval modulation for optical communications," *IEEE Commun. Mag*, vol. 36, no. 12, pp. 95–99, Dec. 1998.

[18] S. Khazraei, M. Shoaie, and M. Pakravan, "Efficient modulation technique for optical code division multiple access networks: Differential pulse position modulation," *IET Optoelectron.*, vol. 8, no. 5, pp. 181–190, Oct. 2014.

[19] B. Bai, Z. Xu, and Y. Fan, "Joint led dimming and high capacity visible light communication by overlapping ppm," in *Proc. 2010 19th Annu. Wireless Opt. Commun. Conf.*, May 2010, pp. 1–5.

[20] M. Noshad and M. Brandt-Pearce, "Expurgated PPM using symmetric balanced incomplete block designs," *IEE Commun. Lett.*, vol. 16, no. 7, pp. 968–971, Jul. 2012.

[21] X. Ma, K. Lee, and K. Lee, "Appropriate modulation scheme for visible light communication systems considering illumination," *Electron. Lett.*, vol. 48, no. 18, pp. 1137–1139, Aug. 2012.

[22] A. Ali, Z. Zhang, and B. Zong, "Pulse position and shape modulation for visible light communication system," in *Proc. 2014 Int. Conf. Electromagn. Adv. Appl.*, Aug. 2014, pp. 546–549.

[23] Y. Zeng, R. Green, and M. Leeson, "Multiple pulse amplitude and position modulation for the optical wireless channel," in *Proc. 2008 10th Anniversary Int. Conf. Transparent Opt. Netw.*, Jun. 2008, vol. 4, pp. 193–196.

[24] X. You, J. Chen, H. Zheng, and C. Yu, "Efficient data transmission using MPPM dimming control in indoor visible light communication," *IEEE Photon. J.*, vol. 7, no. 4, pp. 1–12, Aug. 2015.

[25] D. shan Shiu and J. Kahn, "Differential pulse-position modulation for power-efficient optical communication," *IEEE Trans. Commun.*, vol. 47, no. 8, pp. 1201–1210, Aug. 1999.

[26] H. Ai-ping, F. Yang-Yu, L. Yuan-Kui, J. Meng, B. Bo, and T. Qing-Gui, "A differential pulse position width modulation for optical wireless communication," in *Proc. 4th IEEE Conf. Ind. Electron. Appl. 2009*, May 2009, pp. 1773–1776.

[27] W. Popoola, E. Poves, and H. Haas, "Spatial pulse position modulation for optical communications," *J. Lightw. Technol.*, vol. 30, no. 18, pp. 2948–2954, Sep. 2012.

[28] T. Ohtsuki, "Multiple-subcarrier modulation in optical wireless communications," *IEEE Commun. Mag.*, vol. 41, no. 3, pp. 74–79, Mar. 2003.

[29] P. Haigh *et al.*, "Multi-band carrier-less amplitude and phase modulation for bandlimited visible light communications systems," *IEEE Wireless Commun.*, vol. 22, no. 2, pp. 46–53, Apr. 2015.

[30] G. Ntogari, T. Kamalakis, J. Walewski, and T. Sphicopoulos, "Combining illumination dimming based on pulse-width modulation with visible light communications based on discrete multitone," *IEEE/OSA Opt. Commun. Netw.*, vol. 3, no. 1, pp. 56–65, Jan. 2011.

[31] A. Mirvakili, V. Koomson, M. Rahaim, H. Elgala, and T. Little, "Wireless access test-bed through visible light and dimming compatible ofdm," in *Proc. IEEE Wireless Commun. Netw. Conf.*, Mar. 2015, pp. 2268–2272.

[32] T. Lueftner, C. Kroepl, M. Huemer, J. Hausner, R. Hagelauer, and R. Weigel, "Edge-position modulation for high-speed wireless infrared communications," *IEE Proc.–Optoelectron.*, vol. 150, no. 5, pp. 427–437, Oct. 2003.

[33] K. Lee and H. Park, "Channel model and modulation schemes for visible light communications," in *Proc. IEEE 54th Midwest Symp. Circuits Syst.*, Aug. 2011, pp. 1–4.

[34] T. Komine and M. Nakagawa, "Fundamental analysis for visible-light communication system using led lights," *IEEE Trans. Consum. Electron.*, vol. 50, no. 1, pp. 100–107, Feb. 2004.

[35] L. W. Couch, II, *Digital and Analog Communication Systems*, 6th ed. Upper Saddle River, NJ, USA: Prentice-Hall, 2000.

[36] D. A. Guimaraes, *Digital Transmission* (ser. Signals and Communication Technology). Berlin: Springer, 2009.

[37] S. Arnon, "The effect of clock jitter in visible light communication applications," *J. Lightw. Technol.*, vol. 30, no. 21, pp. 3434–3439, Nov. 2012.

[38] R. Gagliardi, "The effect of timing errors in optical digital systems," *IEEE Trans. Commun.*, vol. 20, no. 2, pp. 87–93, Apr. 1972.

[39] K. Lee and H. Park, "Modulations for visible light communications with dimming control," *IEEE Photon. Technol. Lett.*, vol. 23, no. 16, pp. 1136–1138, Aug. 2011.

Nobby Stevens (M'14) received the Master's degree in physical engineering from Ghent University, Gent, Belgium, in 1997, the DEA degree from the Institut National Polytechnique de Grenoble, Grenoble, France, in 1997, and the Ph.D. degree from Ghent University, in 2004. From the end of 1997 to August 1998, he was a Product Development Engineer with Philips. Beginning in August 1998, he performed research on numerical modeling of electromagnetic fields interacting with the human body with the Department of Information Technology, Ghent University. In June 2004, he joined Agilent EEsof, Santa Rosa, CA, USA, as a Research and Development Engineer where he was involved with computational electromagnetics. Since November 2008, he has performed research with the DraMCo (wireless and mobile communications) group, ESAT, KU Leuven, Ghent, Belgium. His research interests include visible light communications and wireless power transfer by inductive coupling.

Lieven De Strycker (M'01) received the Master's and Ph.D. degrees in electrotechnical engineering from Ghent University, Ghent, Belgium, in 1996 and 2001, respectively. Since 2001, he has been a Professor with the Catholic University College Ghent, Ghent, Belgium, where he founded, with his colleagues, the DraMCo (wireless and mobile communications) Research Group. Since 2008, he has been an Associated Professor with the Katholieke Universiteit Leuven, Leuven, Belgium.